NASA Technical Memorandum 83786

Fracture Surface Characteristics of Notched Angleplied Graphite/Epoxy Composites

Carol A. Ginty and Thomas B. Irvine
Lewis Research Center
Cleveland, Ohio

Prepared for the
International Symposium—Composites: Materials and Engineering
sponsored by the Center for Composite Materials, The University of Delaware
Newark, Delaware, September 24-28, 1984

NASA

FRACTURE SURFACE CHARACTERISTICS OF NOTCHED ANGLEPLIED GRAPHITE/EPOXY COMPOSITES

Carol A. Ginty* and Thomas B. Irvine*

National Aeronautics and Space Administration
Lewis Research Center
Cleveland, Ohio 44135

SUMMARY

Composite fracture surface characteristics and related fracture modes have been investigated through extensive microscopic inspections of the fracture surfaces of notched angleplied graphite/epoxy laminates. The investigation involved 4 ply G/E laminates of the configuration $[\pm\theta]_S$ where θ = 0°, 3°, 5°, 10°, 15°, 30°, 45°, 60°, 75°, and 90°. Two-inch wide tensile specimens with 0.25 in. by 0.05 in. throughslits centered across the width were tested to fracture. The fractured surfaces were then removed and examined using an Amray 1200 Scanning Electron Microscope (SEM).

Evaluation of the photomicrographs combined with analytical results obtained using the CODSTRAN computer code have culminated in a unified set of fracture criteria for determining the mode of fracture in notched angleplied graphite/epoxy laminates.

INTRODUCTION

An extensive microscopic investigation has been conducted on the fracture surfaces of graphite/epoxy (G/E) composite laminates. This investigation is part of a larger on-going "Composite Fracture Characterization" program at the NASA Lewis Research Center. The purpose of this study was to develop a set of fracture surface characteristic criteria in order to determine the associated fracture mode.

The composite system used in the investigation consisted of 4-ply G/E laminates with a $[\pm\theta]_S$ configuration. Two-inch wide tensile specimens including: a) solid coupon-type, b) notched with centered through-slits, and c) notched with centered through-holes were tested to fracture. A portion of the fracture surface was removed for microscopic examination. Although all the laminate fracture surfaces were examined, only the characteristics of the notch/slit specimens are presented here, since the slit geometrically resembles a crack which is a subject of great concern in composite structural design.

Using an Amray 1200 scanning electron microscope, the fracture surfaces of the notch/slit specimen were observed and the microstructural fracture surface characteristics were captured on photomicrographs at varying degrees of magnification. Evaluation of the photomicrographs served as a basis for formulating a set of microstructural fracture mode criteria for notched angleplied G/E composites.

---

*Aerospace Structures Engineers.

In conjunction with the SEM evaluations, an independent analytical investigation was conducted using the CODSTRAN (COmposite Durability STRuctural ANalysis), computer code. CODSTRAN is an integrated computational capability developed at the NASA Lewis Research Center to predict defect growth and fracture of composite structures. By using the predictive capabilities of CODSTRAN, the microstructural characteristics - fracture mode relationship developed by the SEM studies was verified.

Procedures for fabricating and testing the laminates, results of the microscopic investigation of the notched specimen fracture surfaces, and the correlation between the SEM determined fracture modes and the CODSTRAN predicted fracture modes are presented and discussed below.

SPECIMEN FABRICATION AND TESTING

The composite laminates consisted of 4 plies of Fiberite 1034E prepreg (934 resin matrix impregnated with Thornel 300 graphite fibers) fabricated into 12 in. by 18 in. panels. Using a diamond tipped cutting wheel, the panels were cut into 18 in. long and 2 in. wide specimens. The full penetration notch (0.25 in. by 0.05 in.) was placed in the center of the specimens with an ultrasonic milling machine using an abrasive slurry. The specimens containing 0.25 in. diameter full penetration holes were machined using a mandrel (core drill), plated with a diamond abrasive. All specimens (solid, notch/slit and notch/hole) were tabbed at the ends with 2 in. wide beveled aluminum tabs. More detailed information on the fabrication process is available in reference 1.

Uniaxial tension testing of the specimens was conducted in an incremental load-to-fracture manner using a 50 kip load frame with a prescribed load increment size. Fracture was catastrophic for the lower angle (0° to 15°) G/E specimens leaving very little of the composite intact (fig. 1(a)). The remaining angleplied specimens (30° to 90°) exhibited a brittle fracture process that produced puzzle-like pieces of the composite as the specimens broke apart (fig. 1(b)). Table I lists the fracture loads of the solid and notched specimens for each laminate configuration in the series.

THE MICROSCOPIC INVESTIGATION

In order to establish a relationship between the microstructural characteristics of the laminate fracture surface and the attendant fracture mode, photomicrographs were obtained of the fracture surfaces of the notch/slit G/E laminates. The results are presented and discussed below.

The photomicrographs document the microscopic investigation conducted using the Amray 1200 Scanning Electron Microscope (SEM). For each laminate in the series, a section of the fracture surface approximately 0.75 in. wide was removed from the specimen for insertion into the SEM. From the notched specimens, the fracture surface section was extracted at or near the original notch. Special care was taken to preserve the fracture surface from the water and debris involved in the diamond wheel cutting process. Having mounted the section onto aluminum seats, the SEM specimens were coated with a 200-Å thick gold film using a vapor deposition process. The gold film enhances the conductivity of the specimen and hence improves the transmission of the SEM.

Three photomicrographs of the fracture surface of each laminate at different levels of magnification were selected as a basis for formulating the fracture characteristics - fracture mode criteria.

The fracture surface characteristics of the notched G/E unidirectional laminate are presented in figure 2. The distinguishing feature of the fracture surface is the tiered fibers (ref. 2) as seen in figure 2(a). This tiered effect is the result of fiber pull-out caused by fibers breaking at various locations along the length of the fiber. Note that the fiber surfaces in figure 2(c) are relatively clean and free of matrix residue. This unidirectional laminate being tested in longitudinal tension will fracture due to a longitudinal tensile mode. Therefore, the microstructural characteristics just described are indicative of a longitudinal tensile fracture mode with the tiered surface being the primary microscopic feature.

At greater magnifications (figs. 2(b) and (c)) a characteristic associated with an intraply shear mode is observed. This characteristic is represented by the presence of matrix debris being squeezed out between the fibers. This characteristic is referred to here as matrix hackles. The amount of matrix hackles present is minimal indicating that even though a shearing mode did exist, its contribution to final fracture was minimal and that the primary mode of fracture for this unidirectional laminate was a longitudinal tensile mode.

The same microstructural characteristics depicted for the unidirectional laminate are observed on the fracture surface of the $[\pm 3]_S$ laminate (fig. 3). Although the characteristics are similar, there is a distinct change in the tier formation. Figures 3(a) and (b) show fiber pull-out and breakage occurring more randomly. This action still produces an irregular fracture surface but without the wall-like formation of each ply that existed for the unidirectional laminate. In figure 3(c), matrix hackles are apparent indicating an intraply shearing action. Nevertheless, final fracture was the result primarily of a longitudinal tensile fracture mode.

Fiber pull-out and breakage is the dominant trait of the $[\pm 5]_S$ fracture surface displayed in figure 4. Although the surface is still irregular, individual fibers appear to be breaking at the same locations along the fiber resulting in a leveling-off effect. Matrix hackles are more evident suggesting that even though longitudinal tension is still the primary mode of fracture, intralaminar shear is becoming a larger contributor to final fracture.

Irregular fracture surface and fiber pull-out are still the outstanding microstructural characteristics for the $[\pm 10]_S$ laminate exhibited in figure 5(a). The photomicrograph in figure 5(b), however, reveals a cluster of fibers with relatively clean surfaces breaking at approximately the same place indicating a combination of longitudinal tensile and intraply shear modes respectively. Figures 5(b) and (c) show matrix hackles appearing in an established pattern between the fibers instead of the random occurrence which was previously observed.

Photomicrographs of the $[\pm 15]_S$ laminate fracture surface are presented in figure 6. The irregular surface (fig. 6(a)) and the clean fibers along with the fiber pull-out (fig. 6(b)) indicate a longitudinal tensile fracture mode. Figure 6(c) reveals not only an abundance of matrix hackles but also matrix debris on the surfaces of the fibers which are now forming a level surface, indicative of an intraply shear fracture mode.

A significant change in the microstructure of the fracture surface is observed in the photomicrographs of the $[\pm 30]_S$ laminate in figure 7. Fibers in the outer plies (+30) are breaking at approximately the same place producing a level surface while the inner plies (-30) are still experiencing fiber pull-out and breakage in different locations. The number of fibers affected by this longitudinal tensile fracture mode is decreasing (fig. 7(b)). At the same time, with the presence of matrix hackles and debris increasing (fig. 7(c)), it appears as though intraply shear is becoming the dominant mode of fracture as the ply angle orientation increases.

The prominence of intraply shear controlling the fracture process is illustrated in figure 8 which displays the fracture surface of the $[\pm 45]_S$ laminate. The outer plies now consist of an entirely level surface. The distinct characteristic of the intralaminar shear mode is clean fiber surfaces surrounded by matrix hackles which is clearly depicted in the magnification of the outer level plies (fig. 8(c)). Figure 8(b) characterizes the longitudinal tensile fracture mode; however, the pulled-out fibers contain much matrix debris indicating the presence of an intraply shear fracture mode which is the primary cause of fracture for this laminate.

The fracture surface of the $[\pm 60]_S$ G/E laminate in figure 9(a) is entirely flat with no sign of fiber pull-out. Some fiber breakage (fig. 9(b)) did occur but in the transverse direction. These microstructural characteristics are indicative of a transverse tensile fracture mode. The extensive presence of matrix hackles exhibited in figure 9(c) represents the intraply shear fracture mode which also induces final fracture in this laminate.

More fiber breakage occurring in the transverse direction on the flat fracture surface of the $[\pm 75]_S$ laminate is shown in figures 10(a) and (b). A new characteristic, matrix cleavage, was observed on this surface and is illustrated in figure 10(c). Matrix cleavage resembles a cutting or hollowing-out of the matrix between relatively clean fibers. The microstructural characteristics of this laminate are the result of a transverse tensile fracture mode.

The final fracture surface to be examined is that of the $[90]_4$ G/E laminate presented in figure 11. The flat fracture surface reveals some fiber breakage in figure 11(a). With the occurrence of extensive matrix cracking, the specimen is beginning to fall apart (fig. 11(b)). Magnification of the specimen's edge exposes the matrix cracking and cleavage which causes the fracture due to a transverse tensile fracture mode.

The microscopic fracture surface characteristics and accompanying fracture modes presented and discussed above are for the notch/slit G/E laminates. The same microscopic examination was conducted for the solid and notch/hole laminates as well. Table II summarizes the fracture modes for all the laminates (solid, slit and hole) based on the SEM observations.

THE ANALYTICAL INVESTIGATION

In addition to the microscopic investigation, an analytical investigation was conducted to corroborate the established microstructural fracture surface characteristic/fracture mode relationship developed by the SEM studies. The analytical tool employed was the CODSTRAN (COmposite Durability STRuctural

ANalysis) computer code, previously developed at the NASA Lewis Research Center (ref. 3).

The CODSTRAN code is an integrated computational capability used to predict defect growth and progressive fracture of composites. The major elements comprising CODSTRAN are shown in the flow chart in figure 12 and include: (1) Executive Module; (2) I/O Module; (3) Analysis Module (ref. 4); (4) Composite Mechanics Module (ref. 5); and (5) Fracture Mechanics Module (ref. 6).

The incremental/iterative solution strategy embedded in CODSTRAN provides the means to predict defect growth/progressive fracture in a composite thereby allowing a quantitative assessment to be made of composite durability. Input to CODSTRAN consists of material and laminate properties including: fiber and matrix properties, geometric and laminate configurations, fiber volume ratios, and environmental conditions. Output includes the ply and laminate level stresses due to mechanical and environmental loading, the fracture load, and mode(s) of fracture for each specimen.

Predicted fracture loads for the solid and notched G/E specimens are summarized in table III. CODSTRAN values range from 45 to 134 percent of the measured loads. For the entire series of specimens, the average predicted value of 80 percent of the measured fracture load is quite satisfactory. Nevertheless, the method by which CODSTRAN predicts fracture loads caused by the stress redistribution at an advancing notch tip is being updated.

The fracture modes predicted by CODSTRAN (table IV) are in excellent agreement with those determined with the SEM observations. A unidirectional and one angleply laminate were selected to illustrate this correlation between the determined and predicted fracture modes.

For the unidirectional ($[0]_4$) G/E laminate, microstructural characteristics of the tiered surface and fiber fracture, observed with the SEM, indicated a longitudinal tensile fracture mode. Some hackles, symbolistic of an intralaminar shear mode, were also observed on the notched laminate fracture surface. CODSTRAN predicted fracture due to a longitudinal tensile mode for the solid and notched specimens. In addition, it also indicated intraply shear occurring around the notch tip during progressive fracture.

For the angleply ($[\pm 45]_S$) laminate, final fracture for the notched specimen was attributed to a combination of both longitudinal tensile and intralaminar shear modes with the shearing mode being dominant. CODSTRAN predicted that the same laminate would fracture due to a combination of interply delamination and intraply shear modes.

The criteria used in CODSTRAN for predicting fracture modes is currently being documented and serves as a reliable verification of the relationship which has been established between the fracture surface microstructural characteristics and the fracture modes.

DISCUSSION

Photomicrographs containing the fracture surface characteristics of all the laminates (solid, notch/slit, and notch/hole) were used for the development

of the microstructural fracture criteria. With this available data, a simultaneous investigation was conducted to determine the effect, if any, of the presence of a defect (notch) and the type of notch (slit or hole) on the fracture mode.

Through the microscopic analysis, it was revealed that neither the presence of a defect nor the type of defect had any affect on the fracture surface microstructural characteristics and thereby the fracture modes. This is illustrated in figure 13 for the unidirectional laminate and in figure 14 for the more complex fracture process of the $[\pm 45]_S$ angleply laminate. As can be seen, the microstructural characteristics are identical for the solid and notched specimens for each laminate. This phenomenon was also present in the CODSTRAN predictions which are listed in table IV. Results for the undirectional and $[\pm 45]_S$ laminates, as well as all the other laminates, indicate that neither the presence of a defect nor the type of defect affect the primary mode of fracture in these G/E $[\pm\theta]_S$ laminates. Therefore, use of the fracture surface of the notch/slit laminate to represent the microstructural characteristics of a particular laminate is valid.

With the use of a scanning electron microscope and a small portion of a laminate fracture surface, very little time was required for the examination and documentation of the fracture surface microstructural characteristics. Having completed an extensive investigation, a set of fracture criteria was developed to relate the fracture surface characteristics to the fracture mode. This criteria can be used with confidence since it has been verified with the computer code, CODSTRAN.

SUMMARY OF RESULTS

The results of this extensive microscopic investigation of the fracture surfaces of the $[\pm\theta]_S$ G/E laminates are as follows:

1. SEM photomicrographs reveal distinct microstructural characteristics for each fracture surface in the G/E series of laminates.

2. The microstructural characteristics have been used to develop a criteria by which to determine the accompanying fracture modes.

3. For the lower angleply laminates ($[0]_4$ to $[\pm 15]_S$), fracture is the result of a longitudinal tensile mode characterized by a tiered surface, fiber pull-out and fiber breakage.

4. Laminates with a layup of $[\pm 30]_S$ to $[\pm 45]_S$, fracture from the combined effect of longitudinal tensile and intralaminar shear modes, characterized by both tiered and level surfaces, fiber pull-out and breakage, and an abundant amount of matrix hackles.

5. The cause of fracture in laminates with a higher angleply orientation ($[\pm 60]_S$ to $[90]_4$) is the transverse tensile mode characterized by level surfaces, matrix cleavage and matrix cracking.

6. Fracture characteristics and thereby related fracture modes are a function of the ply angle orientation.

7. The method of relating microstructural characteristics to fracture modes is a valid one which has been verified by CODSTRAN.

8. Neither the presence of a defect (notch) nor the type of defect (slit or hole) affect the fracture surface microstructural characteristics of the $[\pm\theta]_s$ G/E laminates.

REFERENCES

1. Irvine, T. B. and Ginty, C. A.: Progressive Fracture of Composites. NASA TM-83701, 1984.

2. Sinclair, J. H. and Chamis, C. C.: Fracture Surface Characteristics of Off-Axis Composites. NASA TM-73700, 1977.

3. Chamis, C. C. and Smith, G. T.: CODSTRAN: Composite Durability Structural Analysis. NASA TM-79070, 1978.

4. McCormick, C. W., (ed.): NASTRAN User's Manual (Level 15). NASA SP-222(01), 1972.

5. Chamis, C. C.: Computer Code for the Analysis of Multilayered Fiber Composites - User's Manual. NASA TN D-7013, 1971.

6. Chamis, C. C.: Failure Criteria for Filamentary Composites. Composite Materials: Testing and Design, ASTM STP 460, 1969, pg. 336-351.

TABLE I. - FRACTURE LOADS (LB) OF $[\pm\theta]_s$ G/E LAMINATES (DETERMINED EXPERIMENTALLY)

Notch type	Ply configuration: $[\pm\theta]_s$; θ in degrees									
	0	3	5	10	15	30	45	60	75	90
Unnotched--solid	8060	6500	5200	4500	3700	2620	900	420	220	260
Notched--thru slit	7820	5500	4940	4160	2750	2150	880	320	180	180
Notched--thru hole	6000	5720	4700	4240	3300	1750	950	360	220	120

TABLE II. - FRACTURE MODES[a] OF $[\pm\theta]_s$ G/E LAMINATES (DETERMINED BY SEM ANALYSIS)

Notch type	Ply configuration: $[\pm\theta]_s$; θ in degrees									
	0	3	5	10	15	30	45	60	75	90
Unnotched--solid	LT	LT S	LT S	LT S	LT S	LT S	S LT	TT S	TT	TT
Notched--thru slit	LT S	LT S	LT S	LT S	LT S	LT S	S LT	TT S	TT	TT
Notched--thru hole	LT S	LT S	LT S	LT S	LT S	LT S	S LT	TT S	TT	TT

[a]LT = Longitudinal tension
TT = Transverse tension
S = Intraply shear

TABLE III. - FRACTURE LOADS (LB) OF $[\pm\theta]_s$ G/E LAMINATES (PREDICTED BY CODSTRAN)

Notch type	Ply configuration: $[\pm\theta]_s$; θ in degrees									
	0	3	5	10	15	30	45	60	75	90
Unnotched--solid	8300	7400	6950	5000	4400	2150	900	400	200	200
Notched--thru slit	4500	3950	3600	2850	2250	1000	425	300	175	150
Notched--thru hole	4700	3850	3500	2700	2150	1100	425	200	150	100

TABLE IV. - FRACTURE MODES[a] OF $[\pm\theta]_s$ G/E LAMINATES (PREDICTED BY CODSTRAN)

Notch type	Ply configuration: $[\pm\theta]_s$; θ in degrees									
	0	3	5	10	15	30	45	60	75	90
Unnotched--solid	LT	LT S[3]	LT S[3]	LT S[3]	I S	S	I S	TT	TT	TT
Notched--thru slit	LT S[1]	LT S	LT S	S	S	I S	I S	I TT S[2]	TT	TT
Notched--thru hole	LT S	LT S	LT S	S	S LT	I S	I S TT	I TT	TT	TT

[a]LT = Longitudinal tension
TT = Transverse tension
S = Intraply shear:
1) Intraply shear occurring around notch tip during progressive fracture
2) Minimal intraply shearing during fracture
3) Some intraply shear occuring near constraints (grips)
I = Interply delamination

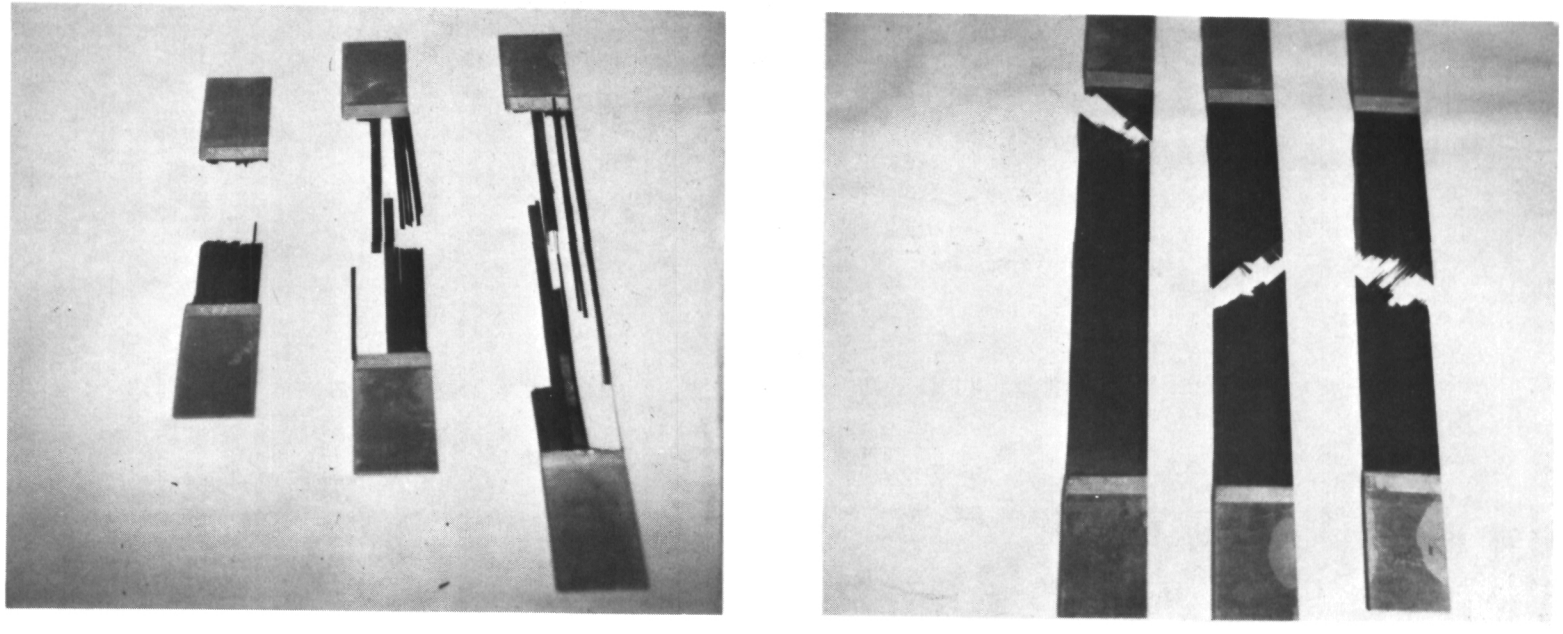

(a) unidirectional.

(b) $[\pm 45]_s$.

Figure 1. - Fractured G/E specimens from left to right -- solid, notch/slit and notch/hole.

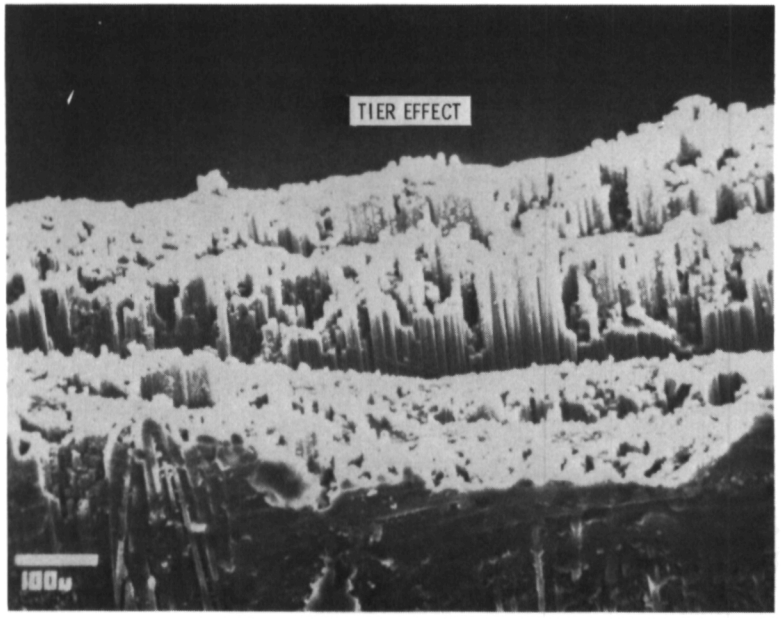

(a) 120X.

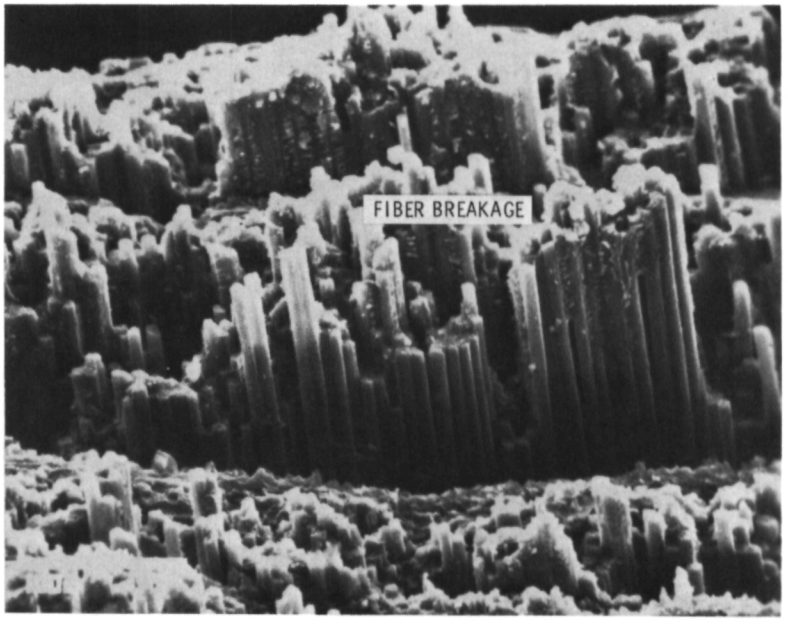

(b) 240X.

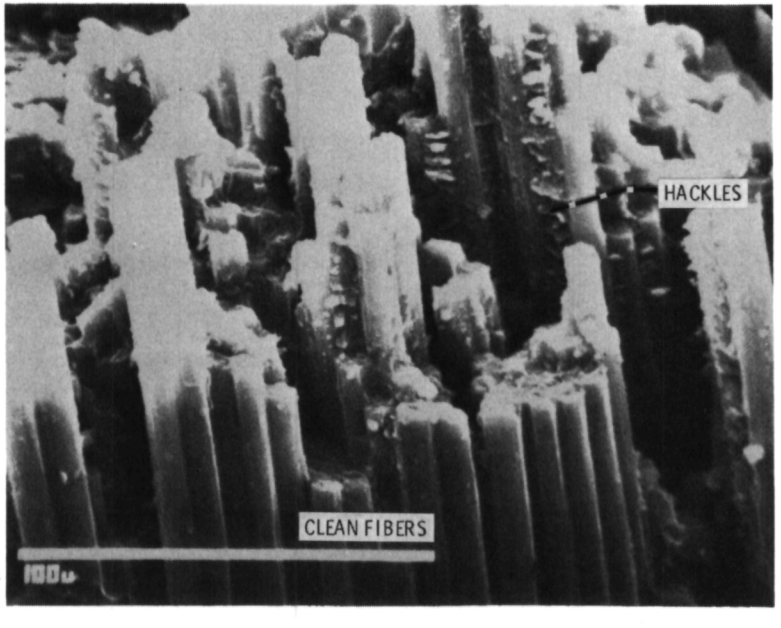

(c) 610X.

Figure 2. - Microstructural fracture surface characteristics of a notch/slit unidirectional G/E laminate. The dominant characteristics are the tiered and pulled-out fibers.

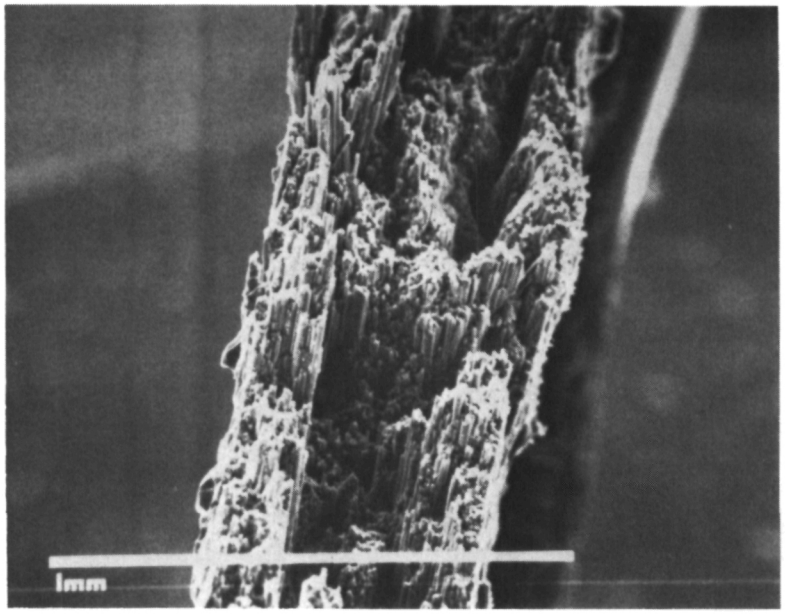

(a) 75X.

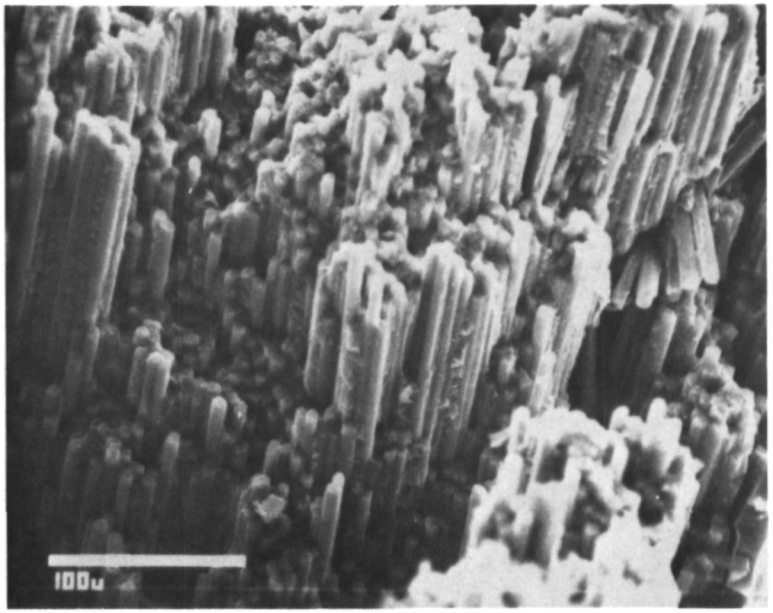

(b) 290X.

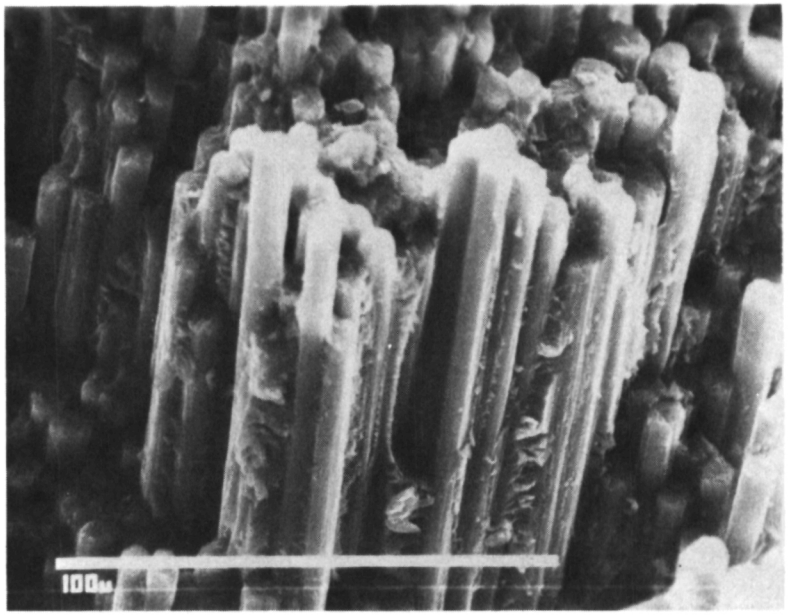

(c)730X.

Figure 3. - Photomicrographs of the [±3]s G/E laminate fracture surface. The predominant characteristic is the fiber breakage.

(a) 120X.

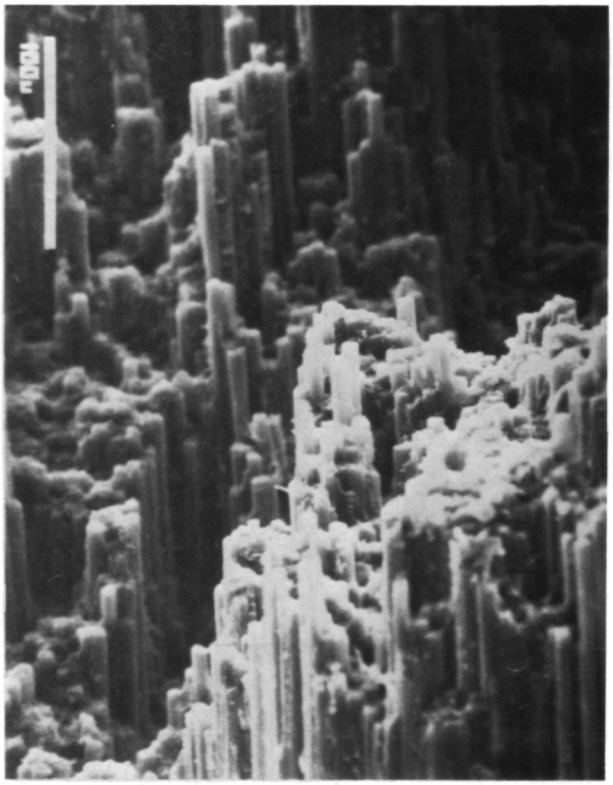

(b) 300X.

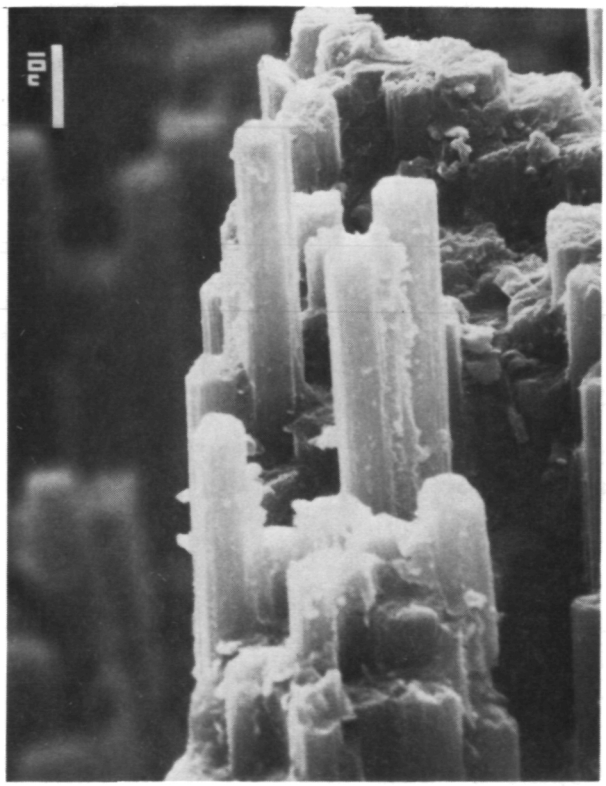

(c)1200X.

Figure 4. - Microstructure of the fracture surface of the [± 5]s G/E laminate revealing fiber breakage accompanied by matrix hackles.

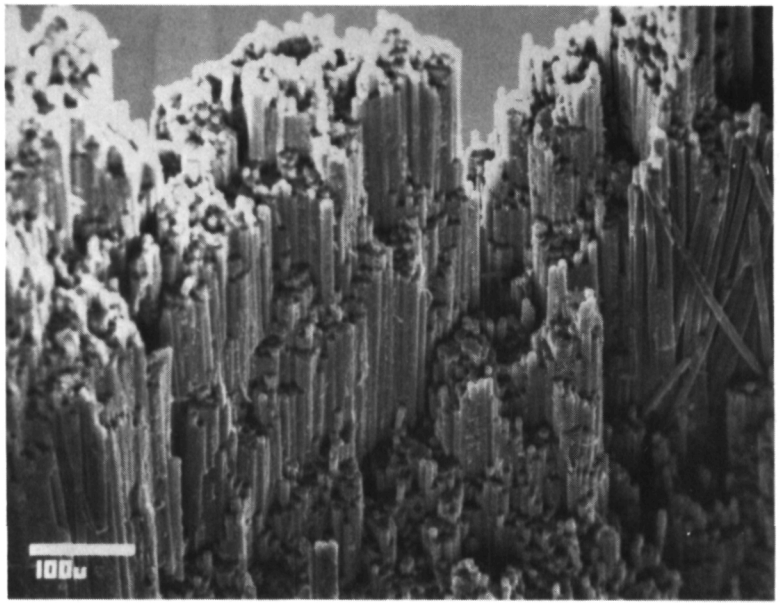

(a) 150X.

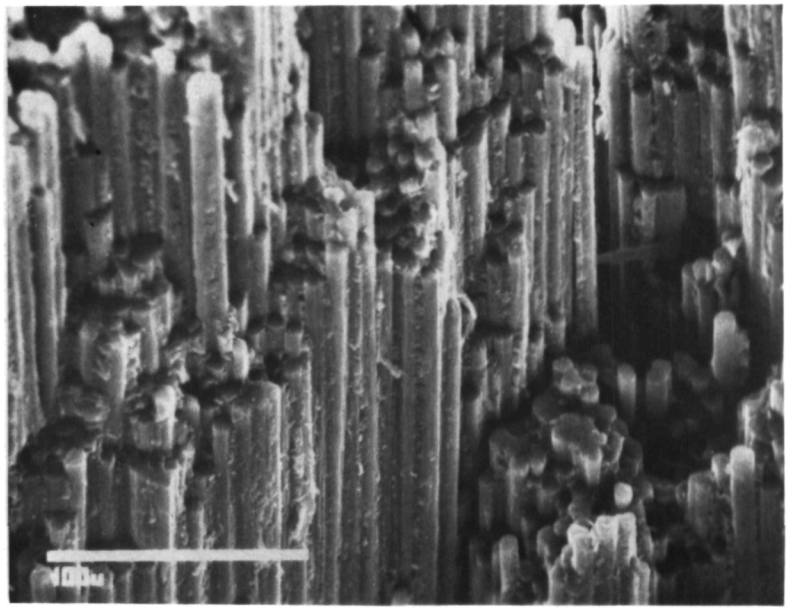

(b) 370X.

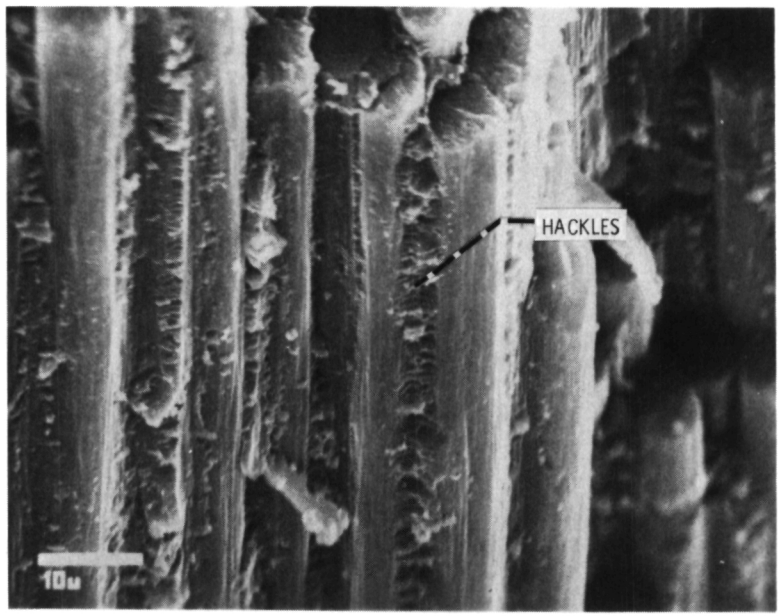

(c) 1500X.

Figure 5. - The fracture surface of the notch/slit [± 10]s G/E laminate revealing matrix hackles between the fibers.

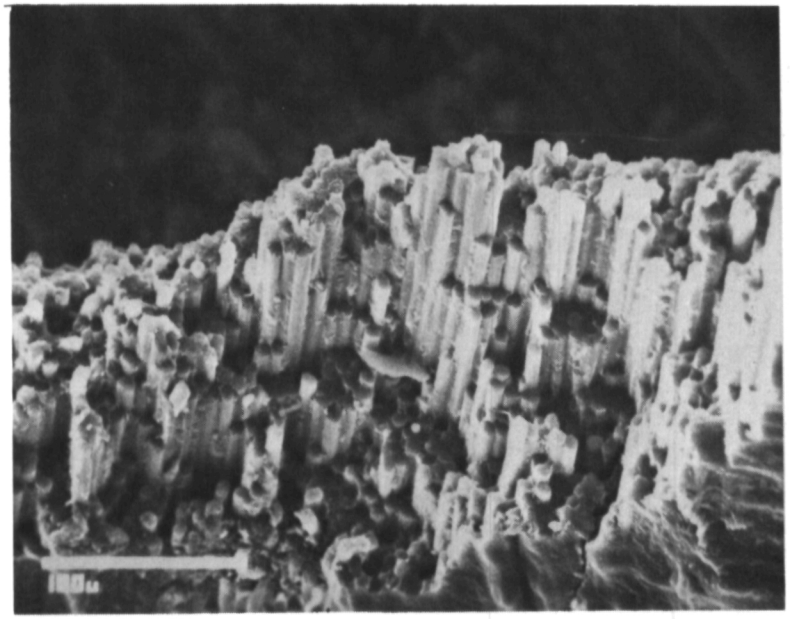

(a) 290X.

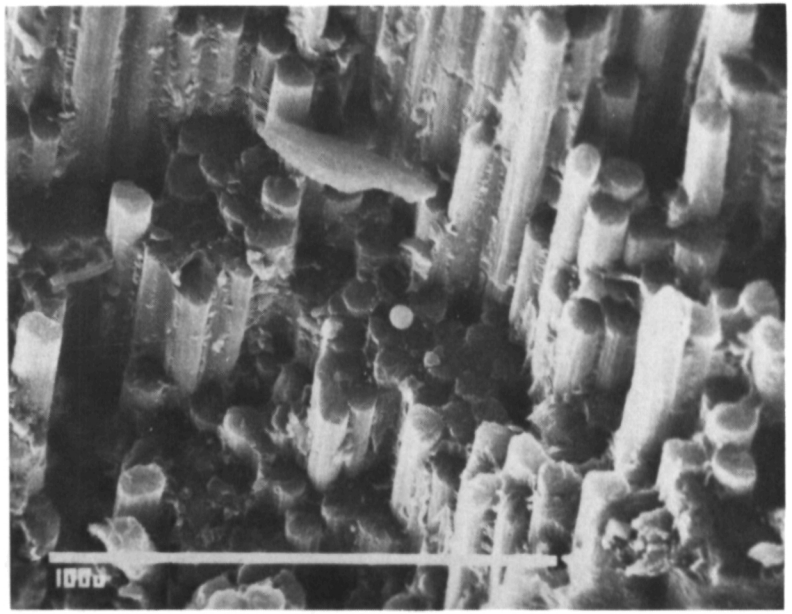

(b) 730X.

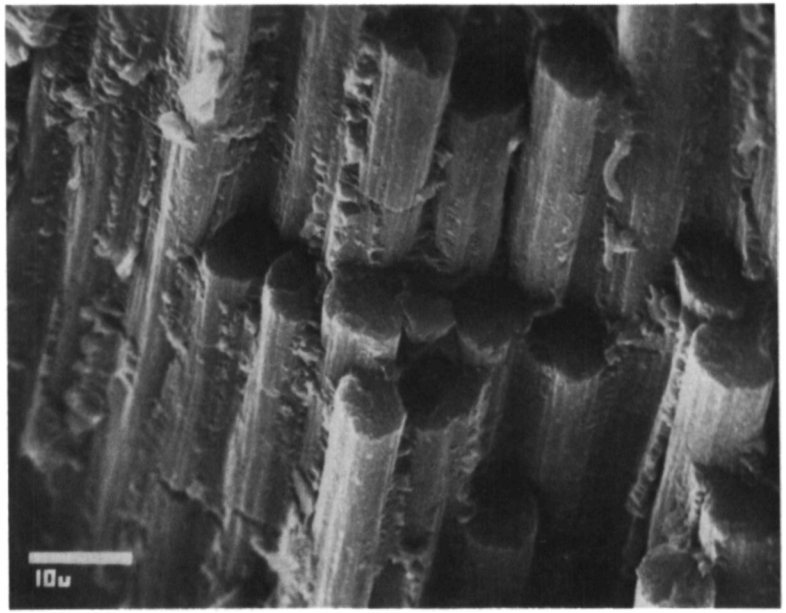

(c) 1500X.

Figure 6. - Photomicrographs revealing the microstructure of the [±15]s G/E fracture surface. Longitudinal tensile and intraply shear fracture modes are characterized by the fiber fracture and matrix hackles respectively.

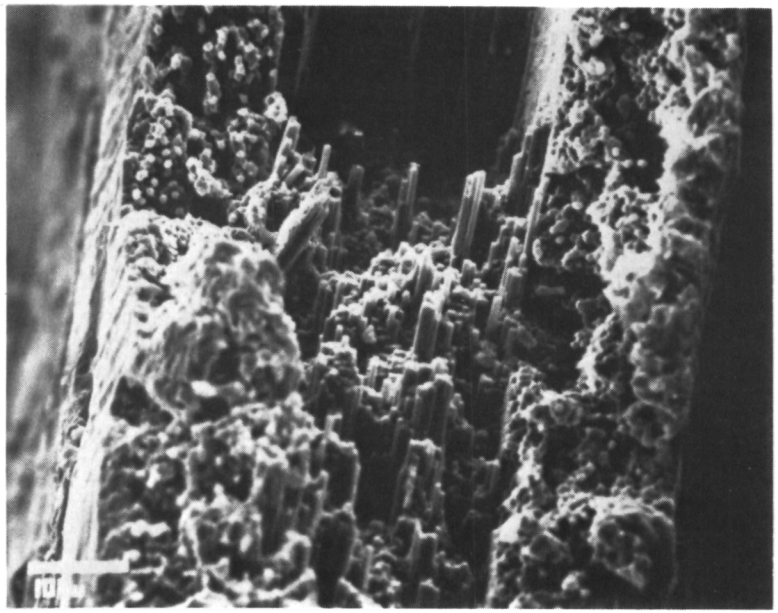

(a) 140X.

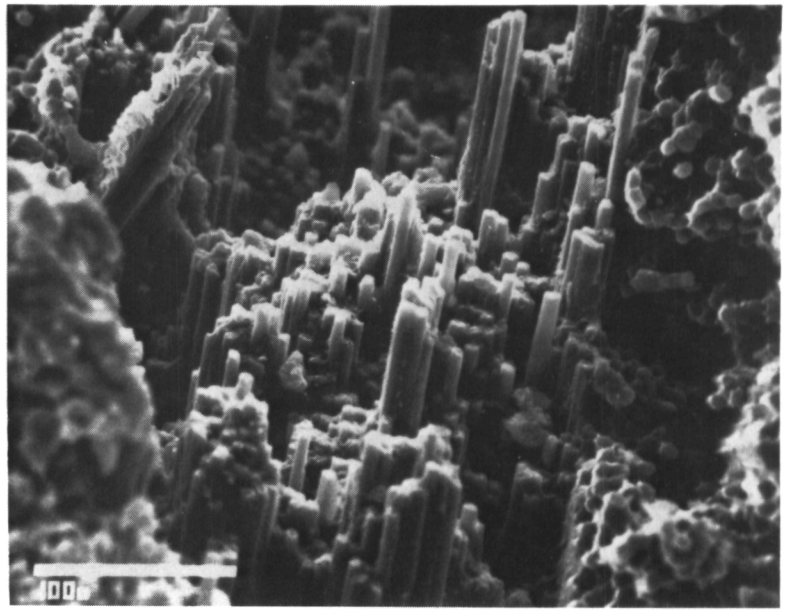

(b) 290X.

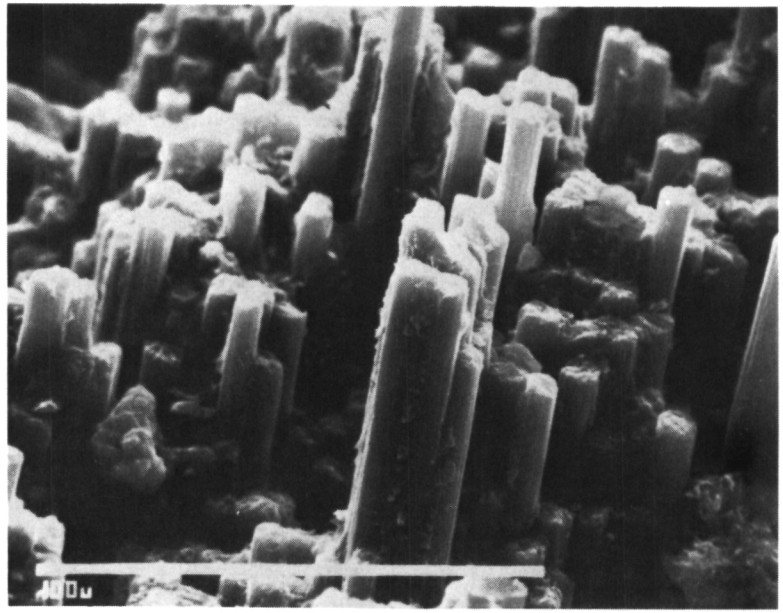

(c) 700X.

Figure 7. - Fracture surface characteristics of the [±30]s notch/slit G/E specimen. The fibers broke at or near the same place producing a more level surface.

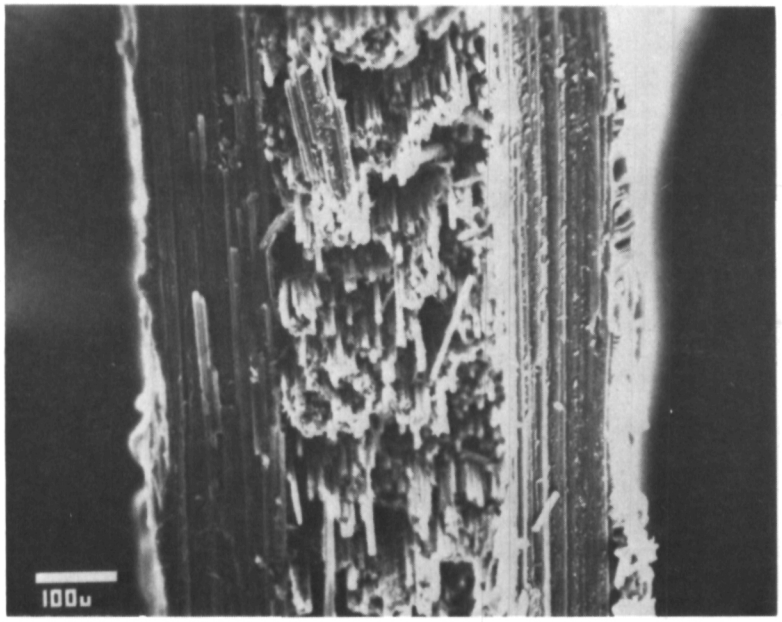

(a) 120X.

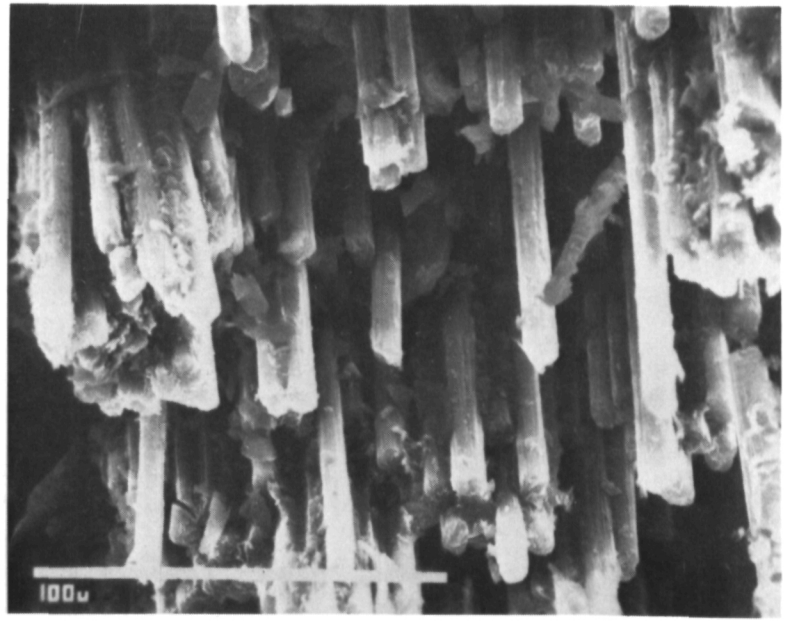

(b) 600X.

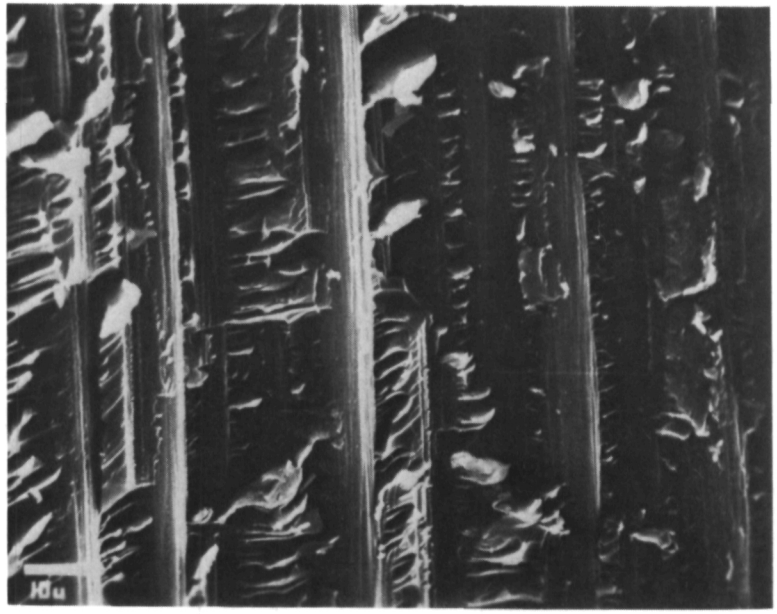

(c) 1200X.

Figure 8. - Photomicrographs depicting the fracture characteristics of the [±45]s G/E laminate. Intralaminar shear fracture designated by matrix debris and hackles is the primary cause of final fracture.

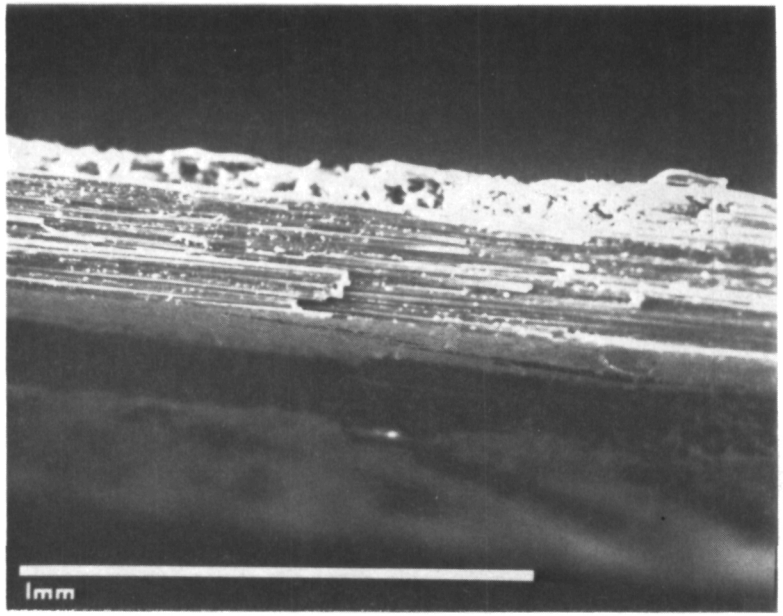

(a) 74 X.

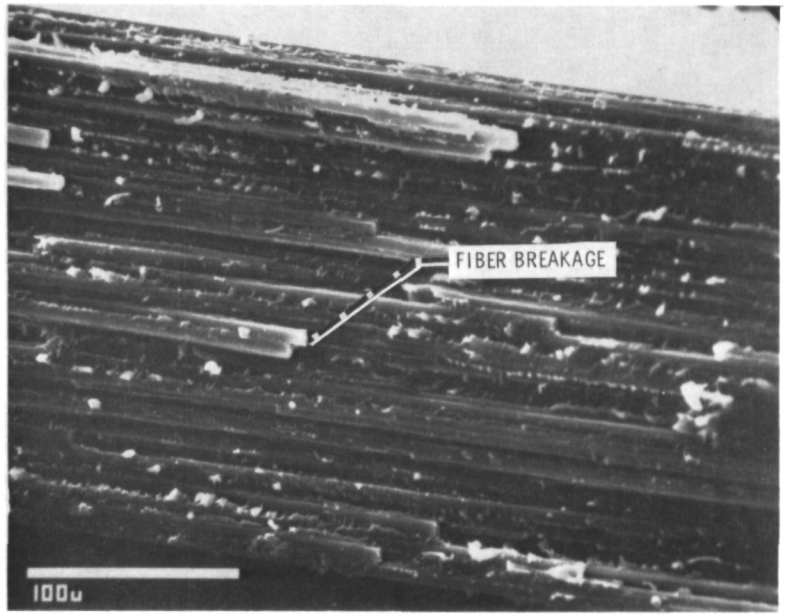

(b) 270 X.

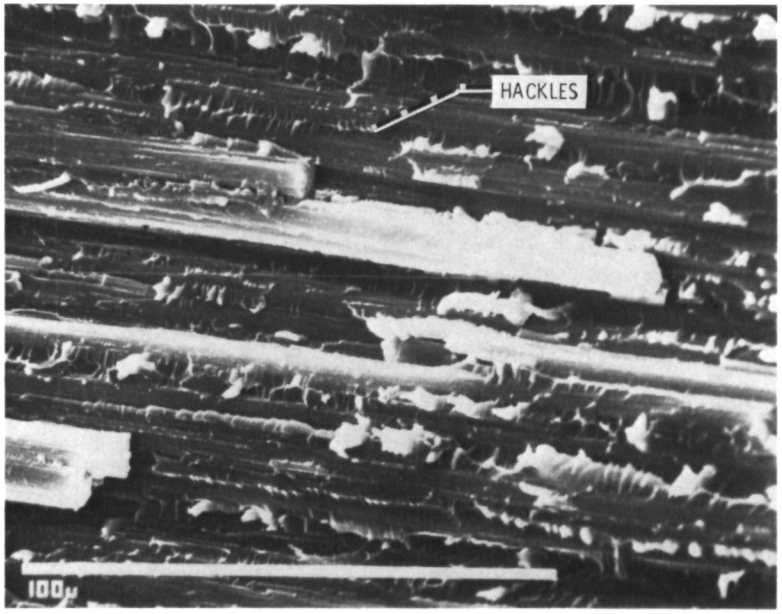

(c) 780X.

Figure 9. - Fracture surface characteristics of the [±60]s G/E laminate. The flat surface is indicative of a transverse tensile mode of fracture.

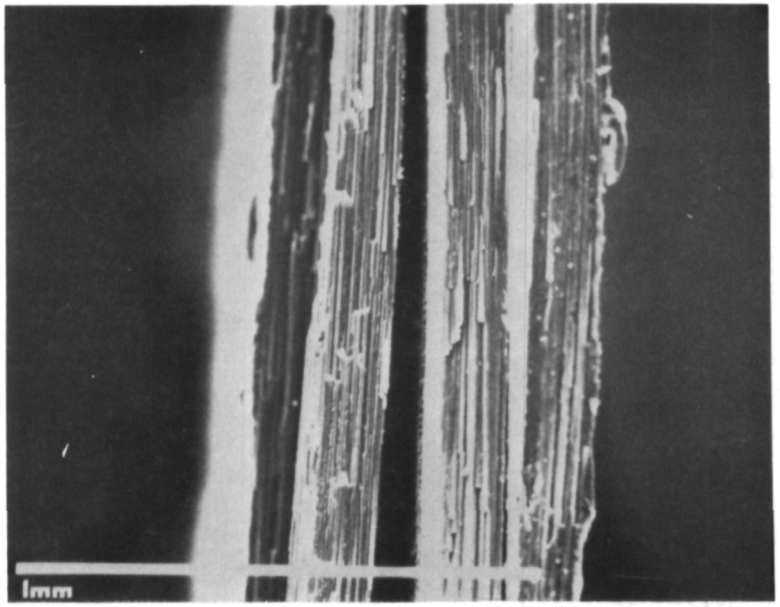

(a) 75X.

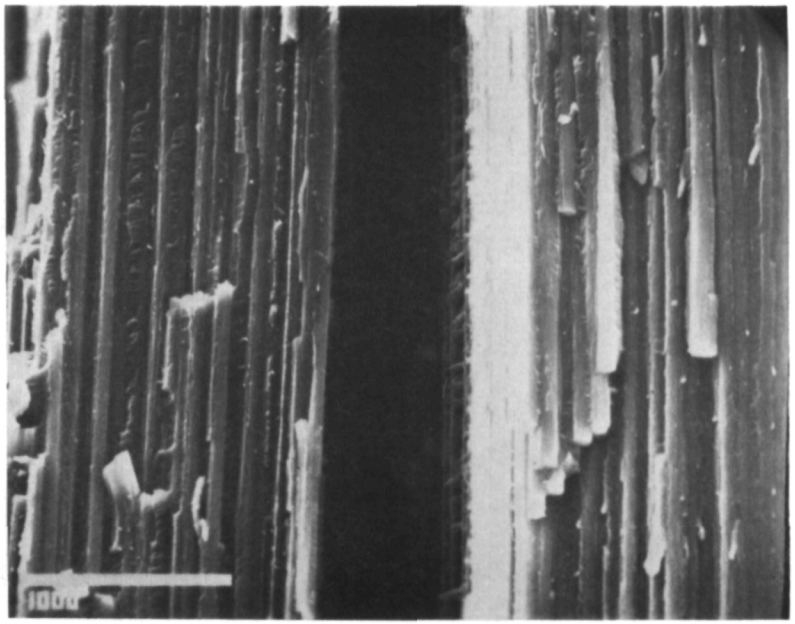

(b) 300X.

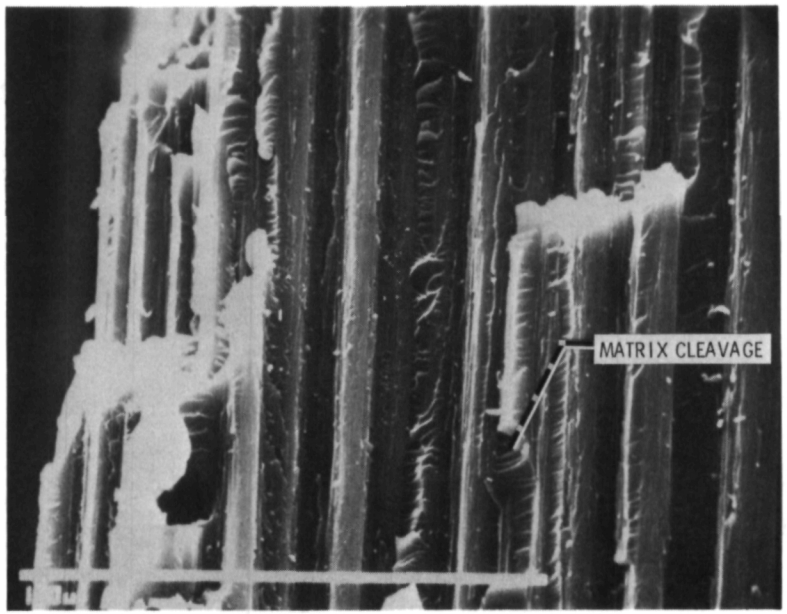

(c) 760X.

Figure 10. - In addition to the flat features, the [±75]s G/E fracture surface consists of fiber fracture and matrix cleavage.

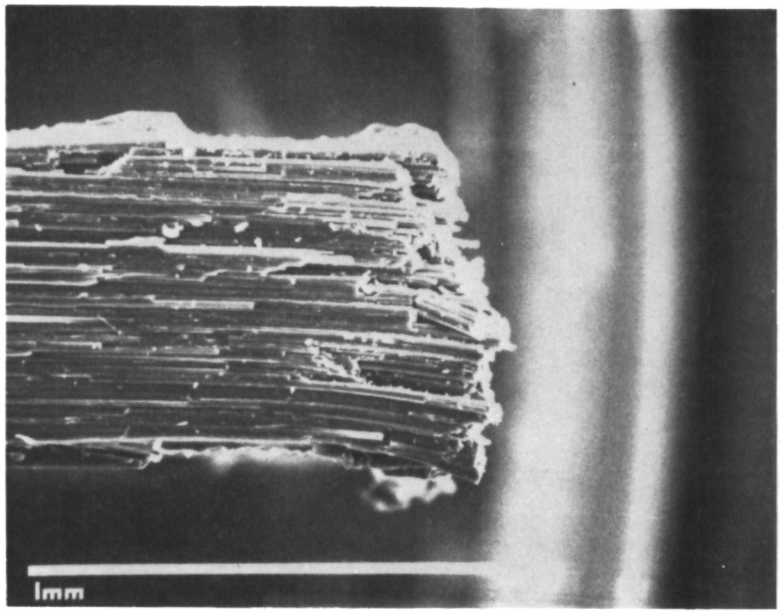

(a) 78X.

(b) 310X.

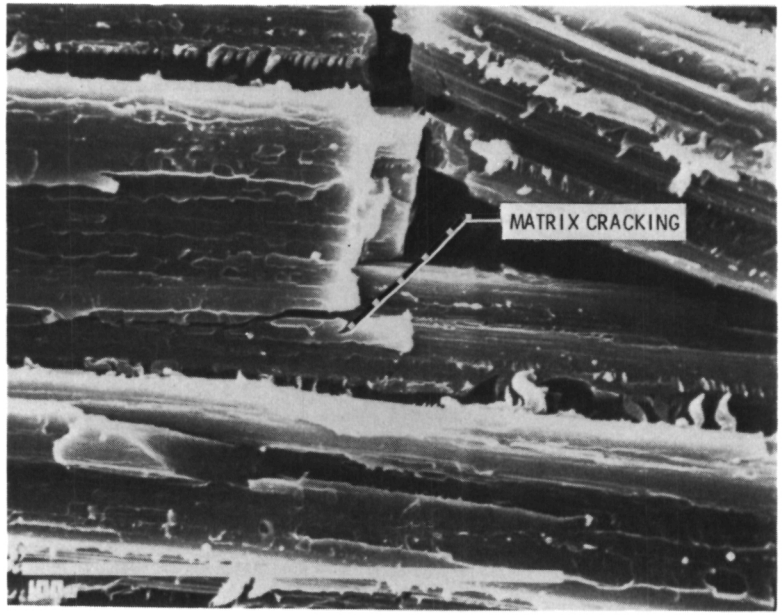

(c) 780X.

Figure 11. - The fracture surface of the notch/slit $[90]_4$ G/E laminate consists of considerable matrix cleavage and cracking.

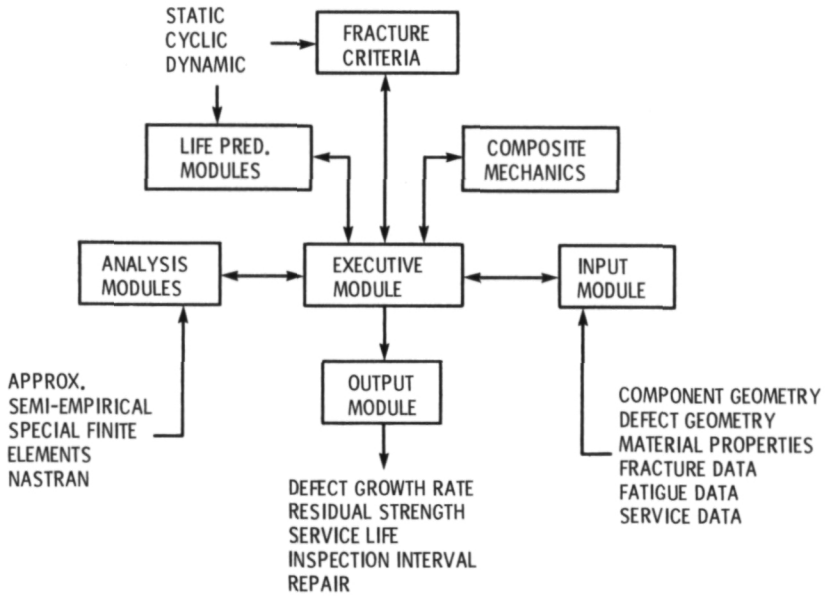

Figure 12. - CODSTRAN flow-chart.

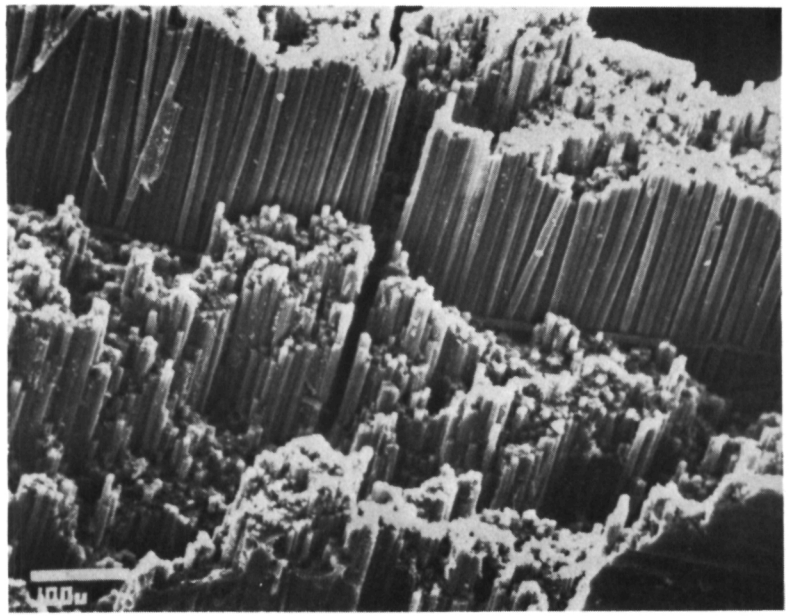

(a) Solid at 140X.

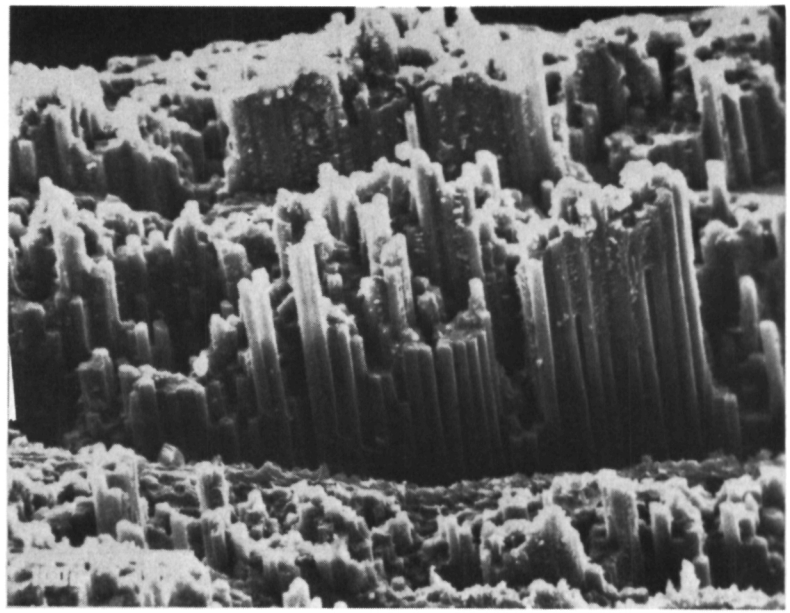

(b) Notch/slit at 240X.

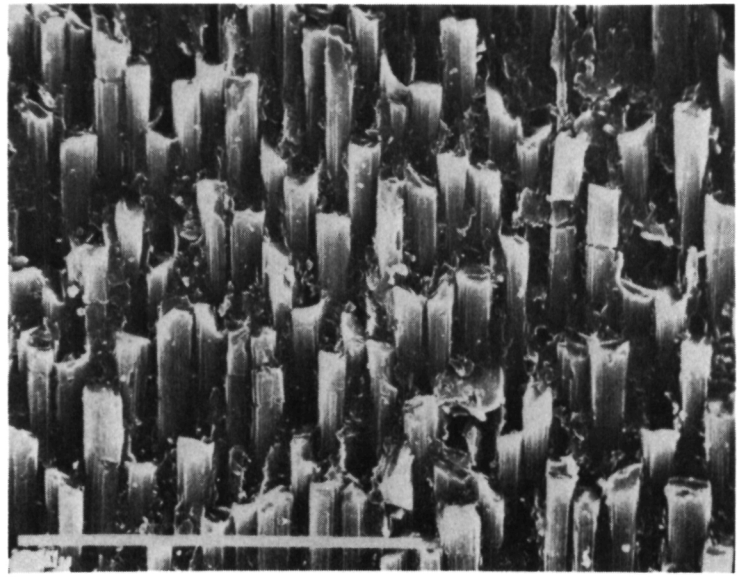

(c) Notch/hole at 250X.

Figure 13. - The microstructural fracture surface characteristics of the unidirectional G/E laminate.

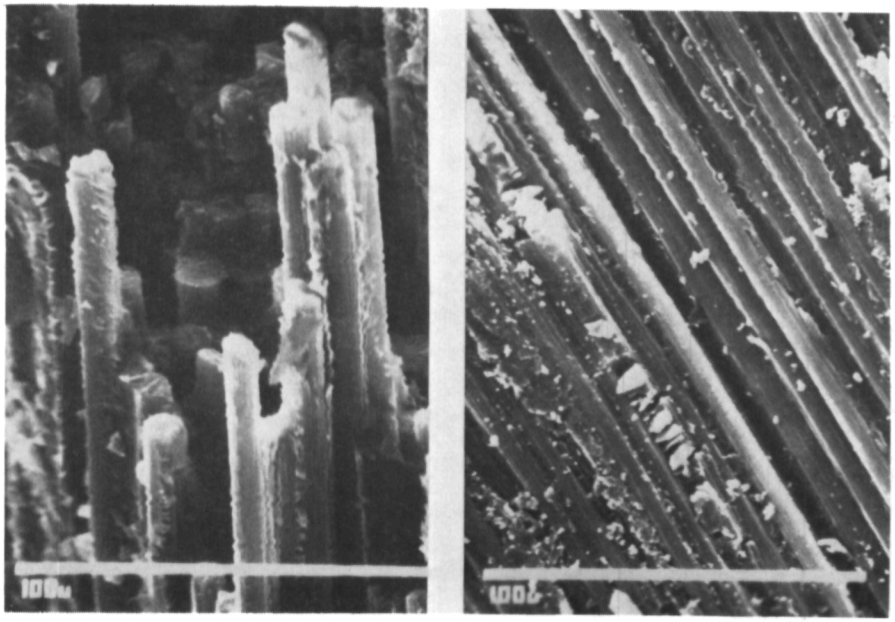

(a) Solid specimen at 710X/560X.

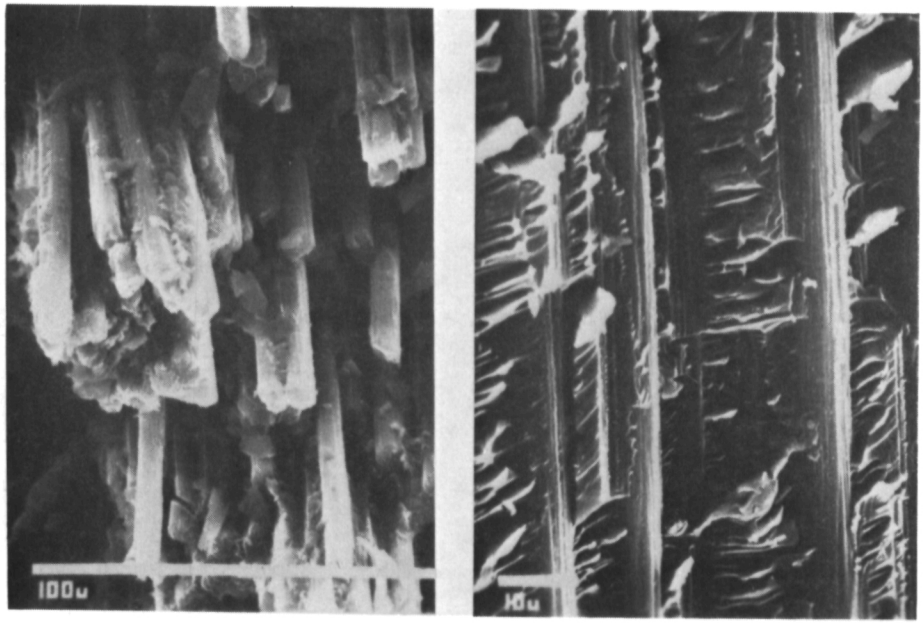

(b) Notch/slit specimen at 600X/1200X.

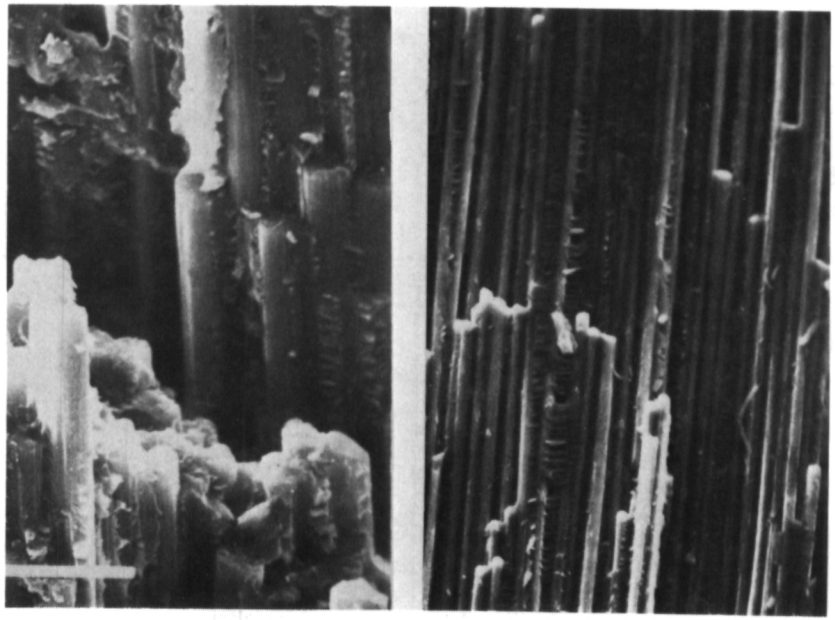

(c) Notch/hole specimen at 730X/200X.

Figure 14. - Fracture surface charateristics of the [±45]s G/E laminate.

1. Report No.	2. Government Accession No.	3. Recipient's Catalog No.
NASA TM-83786		

4. Title and Subtitle	5. Report Date
Fracture Surface Characteristics of Notched Angleplied Graphite/Epoxy Composites	6. Performing Organization Code: 505-33-5B

7. Author(s)	8. Performing Organization Report No.
Carol A. Ginty and Thomas B. Irvine	E-2284
	10. Work Unit No.

9. Performing Organization Name and Address	11. Contract or Grant No.
National Aeronautics and Space Administration Lewis Research Center Cleveland, Ohio 44135	13. Type of Report and Period Covered: Technical Memorandum

12. Sponsoring Agency Name and Address	14. Sponsoring Agency Code
National Aeronautics and Space Administration Washington, D.C. 20546	

15. Supplementary Notes

Prepared for the International Symposium - Composites: Materials and Engineering sponsored by the Center for Composite Materials, The University of Delaware, Newark, Delaware, September 24-28, 1984.

16. Abstract

Composite fracture surface characteristics and related fracture modes have been investigated through extensive microscopic inspections of the fracture surfaces of notched angleplied graphite/epoxy laminates. The investigation involved 4 ply G/E laminates of the configuration $[\pm\theta]_S$ where $\theta = 0^\circ$, 3°, 5°, 10°, 15°, 30°, 45°, 60°, 75°, and 90°. Two-inch wide tensile specimens with 0.25 in. by 0.05 in. through-slits centered across the width were tested to fracture. The fractured surfaces were then removed and examined using an Amray 1200 Scanning Electron Microscope (SEM). Evaluation of the photomicrographs combined with analytical results obtained using the CODSTRAN computer code have culminated in a unified set of fracture criteria for determining the mode of fracture in notched angleplied graphite/epoxy laminates.

17. Key Words (Suggested by Author(s))	18. Distribution Statement
Graphite/epoxy composite; Fracture; Scanning electron microscope; Microstructural surface characteristics; Fracture mode; Fracture criteria	Unclassified - unlimited STAR Category 24

19. Security Classif. (of this report)	20. Security Classif. (of this page)	21. No. of pages	22. Price*
Unclassified	Unclassified		

*For sale by the National Technical Information Service, Springfield, Virginia 22161

National Aeronautics and
Space Administration

Washington, D.C.
20546

Official Business
Penalty for Private Use, $300

SPECIAL FOURTH CLASS MAIL
BOOK

Postage and Fees Paid
National Aeronautics and
Space Administration
NASA-451

NASA

POSTMASTER: If Undeliverable (Section 158
Postal Manual) Do Not Return